8200–8213 *Nucleic Acids Research, 2014, Vol. 42, No. 13* *Published online 10 July 2014*
doi: 10.1093/nar/gku589

SURVEY AND SUMMARY

Reverse gyrase—recent advances and current mechanistic understanding of positive DNA supercoiling

Pavel Lulchev and Dagmar Klostermeier*

University of Muenster, Institute for Physical Chemistry, Corrensstrasse 30, D-48149 Muenster, Germany

Received April 26, 2014; Revised June 16, 2014; Accepted June 22, 2014

ABSTRACT

Reverse gyrases are topoisomerases that introduce positive supercoils into DNA in an ATP-dependent reaction. They consist of a helicase domain and a topoisomerase domain that closely cooperate in catalysis. The mechanism of the functional cooperation of these domains has remained elusive. Recent studies have shown that the helicase domain is a nucleotide-regulated conformational switch that alternates between an open conformation with a low affinity for double-stranded DNA, and a closed state with a high double-stranded DNA affinity. The conformational cycle leads to transient separation of DNA duplexes by the helicase domain. Reverse gyrase-specific insertions in the helicase module are involved in binding to single-stranded DNA regions, DNA unwinding and supercoiling. Biochemical and structural data suggest that DNA processing by reverse gyrase is not based on sequential action of the helicase and topoisomerase domains, but rather the result of an intricate cooperation of both domains at all stages of the reaction. This review summarizes the recent advances of our understanding of the reverse gyrase mechanism. We put forward and discuss a refined, yet simple model in which reverse gyrase directs strand passage toward increasing linking numbers and positive supercoiling by controlling the conformation of a bound DNA bubble.

INTRODUCTION

This year marks the 30th anniversary of the discovery of reverse gyrase. In 1984, a peculiar enzyme was isolated from the thermophilic archaeon *Sulfolobus acidocaldarius* (1) that catalyzed the adenosine triphosphate (ATP)-dependent introduction of positive supercoils into DNA, a reaction hitherto unknown to occur (2–4). Formally, this reaction is opposite to negative DNA supercoiling catalyzed by gyrase (5), and the enzyme was therefore dubbed reverse gyrase. In contrast to the heterotetrameric gyrase that belongs to the type IIA family of topoisomerases, reverse gyrase turned out to be a monomeric type IA topoisomerase that positively supercoils DNA by increasing the linking number (Lk) in steps of +1 (2,3). Reverse gyrases were subsequently identified in and isolated and characterized from other Archaea, such as *Sulfolobus shibatae* (3,6,7) *Sulfolobus solfataricus* (8), *Pyrococcus furiosus* (9), *Methanopyrus kandleri* (10–12), *Archaeoglobus fulgidus* (13–15), *Nanoarchaeum equitans* (16) and *Pyrobaculum calidifontis* (17). Reverse gyrase is also present in hyperthermophilic eubacteria, such as *Calderobacterium hydrogenophilum* (18), *Thermoanaerobacter tengcongensis* (19) and *Thermotoga maritima* (20), and a reverse gyrase-like gene has been identified on a *Thermus thermophilus* plasmid (21). Structurally and functionally, the best-characterized reverse gyrases are the *A. fulgidus* (13–15,22) and *T. maritima* enzymes (20,23–31).

All reverse gyrases isolated and characterized to date catalyze ATP-dependent positive supercoiling of DNA *in vitro*. Although this reaction is considered the hallmark reaction of reverse gyrase, it is unclear whether positive DNA supercoiling is its *in vivo* function. Positive supercoiling of DNA was originally believed to be required for the protection of DNA at high temperatures. A reverse gyrase knockout strain of *Thermococcus kodakaraensis* is viable, but thermosensitive (32), supporting a role of reverse gyrase at high temperatures. However, positive supercoiling does not efficiently protect DNA from thermodenaturation or thermodegradation (33). Also, the presence of reverse gyrase is not correlated with positive supercoiling of DNA *in vivo*. Plasmids from thermophiles and hyperthermophiles that contain reverse gyrase are generally relaxed, with superheli-

*To whom correspondence should be addressed. Tel: +49 251 83 23410; Fax: +49 251 83 29138; Email: dagmar.klostermeier@uni-muenster.de

cal densities of −0.015 to 0.013 (34), while plasmids from mesophilic organisms that lack a reverse gyrase are negatively supercoiled, and have superhelical densities of −0.048 to −0.068 (34). The thermophilic *Methanobacterium thermotrophicum* lacks reverse gyrase and gyrase, yet plasmids are relaxed *in vivo* (34). On the other hand, reverse gyrase and gyrase are present simultaneously in *T. maritima* and *A. fulgidus*, but their plasmids are negatively supercoiled (35,36). Thus, the presence of reverse gyrase does not appear to be linked to positively supercoiled DNA in the cell.

Reverse gyrase is the only enzyme known so far that is exclusively found in hyperthermophiles (21,37), consistent with an important function at high temperatures. A number of observations support a role of reverse gyrase in DNA protection and repair. Reverse gyrase acts as a DNA renaturase that catalyzes annealing of complementary single-stranded DNA circles (38). Plasmids containing single-stranded bubbles are efficiently supercoiled by reverse gyrase, implicating the enzyme in the sensing and elimination of unpaired regions (38). Independent of its supercoiling function, reverse gyrase accumulates around nicks, prevents DNA breakage, and allows for efficient repair (39). Reverse gyrase is degraded after treatment of *S. solfataricus* with alkylating agent, parallel to the degradation of genomic DNA (40). Furthermore, reverse gyrase interacts with and inhibits a translesion polymerase in *S. solfataricus*, depending on its adenosine triphosphatase (ATPase) and topoisomerase activities (41). Reverse gyrase is recruited to DNA after ultraviolet irradiation, and functionally interacts with single-strand DNA binding protein (41), linking reverse gyrase to the cell response to DNA damage (42).

Reverse gyrases are typically monomeric, and consist of an N-terminal helicase module and a C-terminal type IA topoisomerase module in a single polypeptide (2,3,43) (Figure 1A and B). Only few reverse gyrases are naturally split, and consist of separate subunits that associate to form the active, heterodimeric enzyme. *N. equitans* reverse gyrase (16) is formed by two subunits comprising the helicase and the topoisomerase module, respectively. In contrast, the topoisomerase domain is split between the two subunits of *M. kandleri* reverse gyrase (10), implying that during evolution this split enzyme appeared after the fusion of helicase and topoisomerase to reverse gyrase had occurred (10,11) (see (44) for a review).

Mechanistic studies on reverse gyrase have focused on the catalysis of positive DNA supercoiling by reverse gyrase *in vitro.* The helicase and topoisomerase domains jointly contribute to this positive DNA supercoiling activity (45). The helicase and topoisomerase modules from *S. solfataricus* (46) and *S. acidocaldarius* (45) reverse gyrases can be isolated, and active reverse gyrase can be re-constituted by mixing. The so-called latch, a small globular domain inserted within the helicase module (Figure 1A–C), has been implicated in communication between the two domains (13–15,23,25,28). However, the molecular basis for the functional cooperation of helicase and topoisomerase modules in positive DNA supercoiling has been difficult to dissect. For example, in *S. solfataricus* reverse gyrase, the ATPase activity of the helicase module is stimulated by the topoisomerase domain (45), whereas the ATPase activity of the *T. maritima* helicase module is attenuated in reverse gyrase (26,29). The picture of the cooperation of helicase and topoisomerase domains in reverse gyrases is therefore only beginning to emerge.

The most recent reviews on reverse gyrase appeared several years ago, and summarize the link of reverse gyrase to hyperthermophilic life (47), evolutionary aspects (44), and the possible roles of reverse gyrase in maintaining genome stability (48). Since the last reviews on structure and mechanism of positive DNA supercoiling by reverse gyrase have appeared in 2007 (49,50), several milestone discoveries have been reported. Concerning the physiological function of reverse gyrase, a direct link of reverse gyrase to DNA repair has been established (41). Mechanistically, it has been demonstrated that the helicase domain of reverse gyrase undergoes a nucleotide-regulated conformational cycle (23,26,29) that is linked to the catalysis of DNA unwinding (24). The role of the latch for DNA binding, and for DNA unwinding and supercoiling has been delineated (23,24,28). The crystal structure of *T. maritima* reverse gyrase has for the first time revealed the arrangement of all structural elements in reverse gyrase, including the functionally important zinc-fingers (25). This review therefore focuses on the recent advances of our understanding of the mechanism of positive DNA supercoiling by *T. maritima* reverse gyrase.

THE STRUCTURE OF REVERSE GYRASE

Overall structure

A common architecture of reverse gyrases has been inferred from sequence homologies (Figure 1A): an N-terminal domain that displays similarity to superfamily 2 (SF2) helicases is fused to a C-terminal domain homologous to bacterial topoisomerase I (43). Crystal structures of reverse gyrase from *A. fulgidus* (*Afu*_rgyr) (13) and *T. maritima* (*Tma*_rgyr) (25) show the helicase and topoisomerase domains arranged in a padlock shape (Figure 1B). The N-terminal helicase module consists of two RecA-like domains (H1, H2). A so-called latch domain is inserted into H2. An insert region in H1 adopts a β-hairpin structure in *A. fulgidus* reverse gyrase, and a helix-loop structure in the *T. maritima* enzyme. Both inserts protrude from the same side of the helicase domain. Different structures of the latch and the insert region in *Afu*_rgyr and *Tma*_rgyr are in agreement with the lack of conservation in sequence and length among reverse gyrases (13,25) (Supplementary Figure S1). The topoisomerase domain of reverse gyrase has a similar architecture to bacterial topoisomerase IA (51). A central hole in the topoisomerase domain corresponds to the 'topoisomerase hole' previously observed in structures of other type IA topoisomerases (51,52). Two zinc-fingers, one at the N-terminus, preceding H1, and one within the topoisomerase-primase (TOPRIM) domain of the topoisomerase module, were disordered in *Afu*_rgyr, but resolved in the *Tma*_rgyr structure (25) (Figure 1D).

The overall domain arrangement is similar in both reverse gyrases, and consistent with electron microscopy studies of *Sulfolobus tokodaii* reverse gyrase (*Sto*_rgyr) (53). The H1 and H2 domains are oriented similarly with respect to each other in an open conformation in *Afu*_rgyr and *Tma*_rgyr (13,25). Superposition of the two structures on

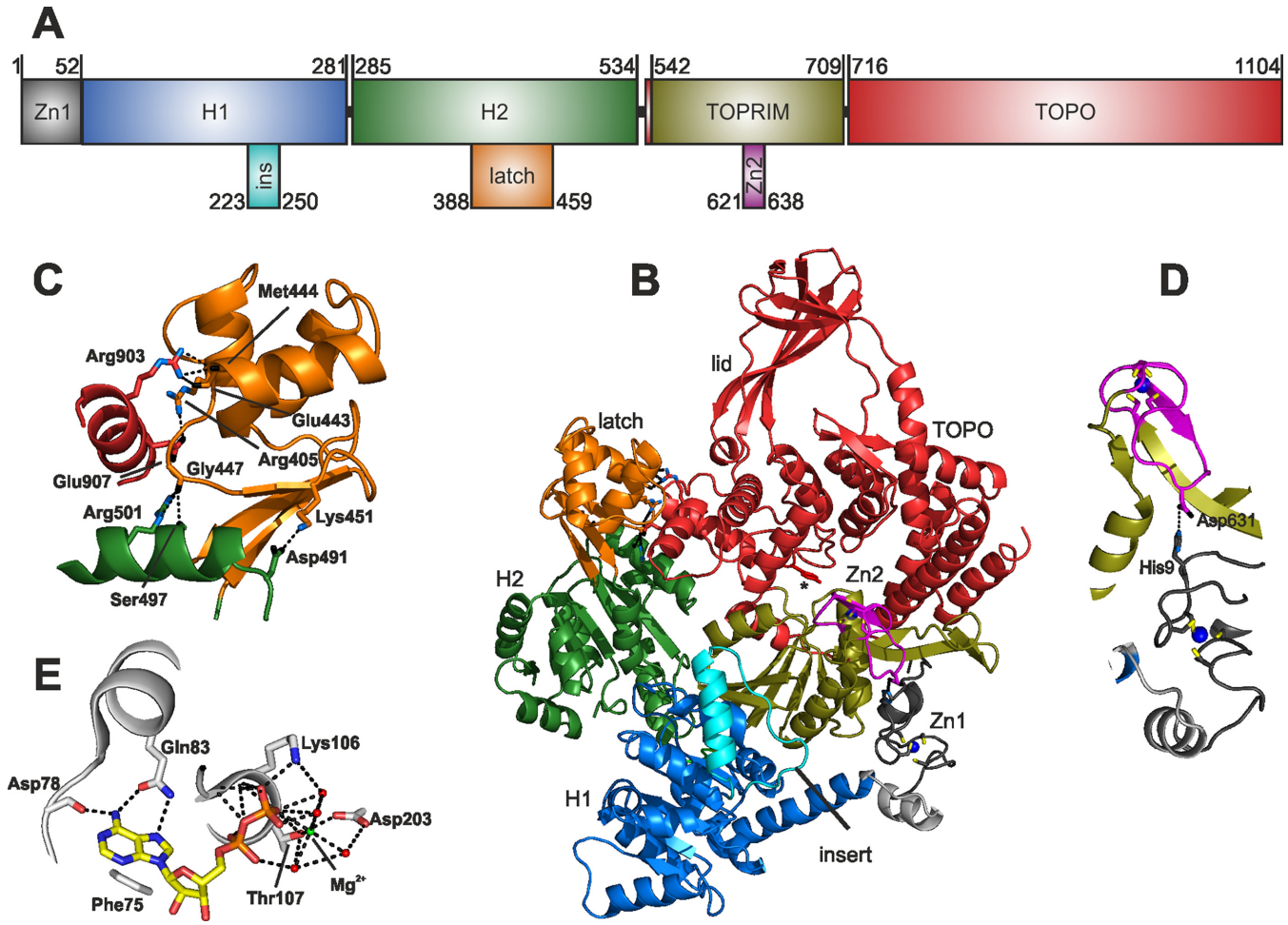

Figure 1. Structure of reverse gyrase. (**A**) Domain architecture of reverse gyrase. Reverse gyrases consist of a helicase module, and a topoisomerase module. The helicase module consists of two flexibly linked RecA-like domains (H1, H2), flanked by an N-terminal zinc finger (Zn1). H1 contains an insert region (ins), and the so-called latch is inserted into H2. The topoisomerase module contains a topoisomerase-primase domain (TOPRIM) that harbors a second zinc finger (Zn2). The numbering refers to reverse gyrase from *Thermotoga maritima*. (**B**) Structure of *T. maritima* reverse gyrase (PDB ID: 4ddu). The elements are depicted in the same color code as in (A). The helicase domain interacts with the TOPRIM domain (H1, Zn1) and Zn2 (Zn1). The part of the topoisomerase domain whose tip interacts with the latch is called the lid. The catalytic tyrosine is shown as stick model and marked by a star. (**C**) Latch–lid interaction. (**D**) Zn1 and Zn2. (**E**) Nucleotide binding site. Broken lines in C-E indicate hydrogen bonds.

the helicase domain shows a relative tilt and shift of their topoisomerase domains, leading to a more than 10 Å displacement of their apexes (25). Comparison of several structures of *Tma*_rgyr in different crystal forms reveals potentially flexible elements, namely the insert in H1, several α-helices within H2 and in the latch, and the apex of the topoisomerase domain. In contrast, the zinc fingers and the core of the topoisomerase domain are invariant in all five structures (25), suggesting that they form a rigid structural scaffold.

The latch

The latch domain has been named in light of its proposed role in the mechanism of positive supercoiling by reverse gyrase (13) (see 'Mechanism of positive DNA supercoiling' section). The latch is inserted into H2 between the conserved Pro387 and the less strictly conserved Pro460 (*Tma*_rgyr numbering, Figure 1A–C, Supplementary Figure S1), and is connected to H2 by a short two-stranded β-sheet with conserved hydrophobic and basic residues. The latch constitutes an independent folding unit, and its deletion does not influence the structure of H2 in *Tma*_rgyr (27,28). The *Afu*_rgyr latch displays structural homology to residues 1–46 of the transcription terminator Rho (13), whereas the *Tma*_rgyr latch shows neither sequence nor structural homology to the latch of *Afu*_rgyr (25) or other proteins. Structural and functional diversity of the latch is expected from little sequence conservation and its substantial variations in length, from 10 amino acids in *Thermosipho africanus* reverse gyrase (*Taf*_rgyr) to 120 amino acids in *P. kodakaraensis* reverse gyrase (25) (Supplementary Figure S1). The latch engages in contacts with the topoisomerase domain, mainly via an α-helix in the topoisomerase domain that is formed by amino acids 856–870 (*Afu*_rgyr) or 901–912 (*Tma*_rgyr, Figure 1C). The interaction surface between latch and the topoisomerase domain is only 745 Å^2 in *Tma*_rgyr, (787 Å^2 in *Afu*_rgyr), in-line with a weak and possibly transient interaction during the cat-

alytic cycle (25). Contacts with the topoisomerase module are mainly established by residues at the base of the latch, and the latch can be tilted without disrupting these interactions (25). Different positions of the latch in different crystal structures of *Tma*_rgyr (25), with a residue displacement of up to 7 Å, further suggest movements of the latch during the reverse gyrase catalytic cycle (25).

Zinc fingers

The two zinc-fingers, at the N-terminus (Zn1) and inserted into the topoisomerase domain (Zn2), were disordered in the *Afu*_rgyr crystal structure (13), but resolved in the *Tma*_rgyr structure (25), demonstrating that they are structured in the absence of DNA (Figure 1B and D). Zn1 forms a Gag-knuckle Zn-finger (54) that coordinates the zinc ion by four cysteines. Zn1 is present in most reverse gyrases, with a core consensus sequence of *Cys*-*Xaa*$_2$-*Cys*-*Xaa*$_{13,14}$-*Cys*-*Xaa*$_{2,7}$-*Cys*, although the size of Zn1 can vary from 30–50 aa (Supplementary Figure S1). Zn1 mediates interactions between the helicase domain and the topoisomerase domain of *Tma*_rgyr, by forming contacts with the TOPRIM domain (Figure 1A and B) that bury ∼1300 Å^2 of surface area (25). Zn2, inserted into the TOPRIM domain, is a ribbon-type Zn-finger (54) that is part of a rigid three-stranded β-sheet emanating from the TOPRIM domain (25). The consensus sequence of Zn2 is *Cys*-*Xaa*$_2$-*Cys*/*His*-*Xaa*$_{10}$-*Cys*-*Xaa*$_2$-*Cys*, although the number of central amino acids varies from as low as 8 (*Desulfobacter*) to 41 (*Pyrolobus*; Supplementary Figure S1). The Zn2 insertion is present in many putative reverse gyrases, but in some cases it is degenerated or missing completely (25) (Supplementary Figure S1). In *Tma*_rgyr, the two zinc-binding motifs are located at the end of the DNA binding cleft close to the catalytic tyrosine in the topoisomerase module (Figure 1B), in a similar position as a protrusion in *Sto*_rgyr that was proposed to contain the zinc fingers (53). Zn1 and Zn2 are connected by an ionic interaction between the side chains of His9 (Zn1) and Asp631 (Zn2) (25) (Figure 1D). The position of the zinc fingers is invariant between different *Tma*_rgyr structures (25).

Nucleotide binding

The nucleotide binding site has been resolved in a structure of the isolated helicase domain of *Tma*_rgyr bound to ADP (27) (Figure 1E). The nucleotide is exclusively bound to H1, and nucleotide binding does not affect the H1–H2 arrangement. The 2′-OH of the ribose is not involved in contacts with the protein, rationalizing why hydroxyl-modified mant-nucleotides are bound by the helicase domain (23,28–30), and why 2′-deoxy-ATP is bound and hydrolyzed by *Afu*_rgyr (15). The adenine base is recognized by the conserved Gln83 that forms a bidentate hydrogen bond with the Hoogsteen face (25). Gln83 is part of a region reminiscent of the Q-motif in DEAD-box helicases (55). Asp78 forms a hydrogen bond with the exocyclic amino group, and Phe75 forms hydrophobic contacts with the aromatic ring (25). Surprisingly, *Afu*_rgyr appears to accept all four NTPs (and dNTPs) as substrates (15), although the adenine-binding residues are conserved (Gln61, Glu56 and Val54 in *Afu*_rgyr). Residues Gly103 and 105, Lys 106 and Thr107 and 108 of *Tma*_rgyr, part of the conserved Walker A motif comprising the P-loop, establish hydrogen bonds to the α- and β-phosphate (25). Comparison of nucleotide-free and nucleotide-bound *Tma*_rgyr helicase domain (25) and *Afu*_rgyr (13) suggests that the P-loop is mobile in the absence of nucleotide, but collapses onto the nucleotide in the bound state. The charge of the β-phosphate is neutralized by Lys106 and by a Mg^{2+} ion (25) that is coordinated by Thr107, four water molecules and Asp203 of the ^{203}DDVD motif. The interaction of Asp203 with the Mg^{2+} ion is analogous to the interaction of the first aspartate of the DEAD-box with the Mg^{2+} ion in the DEAD-box helicase eIF4A-III (56,57). Thr107 of the P-loop forms a hydrogen bond with Asp203, thereby directly linking the P-loop and the DDVD motif (25), again similar to DEAD-box proteins. Thus, the interaction network around the nucleotide bound to *Tma*_rgyr recapitulates the salient features of DEAD-box proteins. The residues involved in adenine nucleotide binding are highly conserved among reverse gyrase, suggesting that the nucleotide binding mode and the specificity for adenine nucleotides are shared by all representatives.

DNA binding

Reverse gyrase contains several putative DNA binding elements. The canonical topoisomerase I DNA binding site is located near the catalytic tyrosine (Y851 in *Tma*_rgyr) in the topoisomerase domain. The helicase core contains a nucleic acid binding site, and contributions of the latch, the insert in H1 and the zinc fingers to DNA binding have been suggested and addressed in mutational studies (19,23–26,28,29,46) (see ‘Mechanism of positive DNA supercoiling’ section). Based on two-dimensional electron micrographs of *Sto*_rgyr bound to double-stranded DNA (dsDNA), models have been proposed where DNA binds along the cleft between H1 and H2 and continues following the long axis of the topoisomerase domain to its apex (53). The electrostatic surface potential of *Afu*_rgyr and *Tma*_rgyr suggests a possible path for DNA across the enzyme, along the contact region of helicase and topoisomerase modules. This path is lined by all putative DNA binding elements (13,25). It is very likely that the binding to DNA changes during the nucleotide cycle of reverse gyrase, with different elements contacting different DNA regions at each step (26,28,29). Such a complex and dynamic recognition of the DNA substrate is intrinsically difficult to dissect. Conformational changes of the (isolated) helicase domain upon DNA and nucleotide binding, leading to a closure of the cleft between H1 and H2, have been demonstrated by single molecule Förster resonance energy transfer (FRET) studies (26), and expand the analogy to DEAD-box proteins (reviewed in (58)). Understanding DNA recognition by reverse gyrase on a molecular and spatio-temporal level requires high-resolution structural information on all intermediates of the nucleotide cycle and information on the kinetics of the inter-conversion of these intermediates in the catalytic cycle of positive DNA supercoiling.

MECHANISM OF POSITIVE DNA SUPERCOILING

Cooperation of a helicase and a topoisomerase

Positive supercoiling of DNA by reverse gyrase requires the functional cooperation of its helicase and topoisomerase domains (45). Early models suggested that the helicase domain may translocate processively along the DNA, leaving negative supercoils in its wake and generating positive supercoils ahead (59). Relaxation of the negative supercoils by the topoisomerase domain *via* a strand passage mechanism, commonly associated with type IA topoisomerases (51), would then lead to positive supercoiling (43). Duplex destabilization upon binding of reverse gyrase to DNA had been demonstrated earlier in the absence of nucleotide (60). Recently, it has been shown that the helicase domain of *Tma*_rgyr and full-length reverse gyrase transiently destabilize a short DNA duplex in an ATP-dependent reaction (24). Unwinding of DNA duplexes by reverse gyrase is not processive, but is reminiscent of the local duplex destabilization by DEAD-box proteins. A second model, the so-called domain model, suggested unwinding of DNA by reverse gyrase, followed by a segregation of underwound and overwound regions. A selective rewinding of the underwound regions by reverse gyrase would then lead to positive supercoiling (45). The molecular basis for topological segregation and for alternating unwinding/rewinding activities has not been elaborated, however. Finally, a nucleotide-dependent regulation of the reverse gyrase affinity for single- and double stranded DNA has been suggested as a basis for selective rewinding of single-stranded regions and for directing strand passage to an increase in linking number and to positive DNA supercoiling (61). In the meantime, the DNA affinities for the different states in the nucleotide cycle of the helicase domain of *Tma*_rgyr have been determined (23,26,29). The helicase domain is indeed a nucleotide-regulated switch, with high affinity for single-stranded DNA (ssDNA) and a preference for single-stranded regions in the ADP state, and high affinity for double-stranded DNA (dsDNA) in the ATP state (29). The switch in (ds)DNA affinities is linked to nucleotide-dependent conformational changes in the helicase domain (26). These studies have lent support to a mechanism based on alternating high affinity binding of ssDNA and dsDNA, and have assigned DNA affinities to the relevant states in the nucleotide cycle. The molecular details of how this affinity switch of the helicase domain is connected to strand passage and supercoiling have yet to be uncovered.

A putative structural model for DNA supercoiling

The crystal structure of *Afu*_rgyr, together with putative models for helicase and topoisomerase IA mechanisms, had inspired a first model for the mechanism of positive DNA supercoiling by reverse gyrases (13). It was proposed that, in a first step, the cleft separating the H1 and H2 domains of the helicase domain would close upon binding of ATP and DNA. As a consequence of the movement of H2 toward H1, the latch would disengage from its interface with the topoisomerase module and release the topoisomerase lid (Figure 1B). One strand of the DNA would be cleaved, mediated by the catalytic tyrosine, and an upward movement of the lid would then provide space for the non-cleaved DNA strand to pass through the gap created in the cleaved opposite strand. Later in the nucleotide cycle, the cleft between H1 and H2 would reopen, and the latch would reestablish interactions with the topoisomerase lid, leading to repression of the topoisomerase module. Religation of the cleaved DNA strand would result in an increase of the DNA linking number by one (13). *Afu*_rgyr does not catalyze DNA relaxation, but gains relaxation activity in the absence of nucleotide upon latch deletion (14,15), in agreement with the suggested repressive role of the latch on the activity of the topoisomerase domain. *Tma*_rgyr also does not relax DNA in the absence of nucleotides, but, in contrast to Afu_rgyr, does not gain relaxation activity when the latch is deleted (28). Thus, the implications of the latch for the activity of the topoisomerase module may differ between different enzymes.

The reverse gyrase helicase domain is a nucleotide-dependent conformational switch

The isolated helicase module has served as an invaluable starting point to dissect the role of the helicase domain for DNA supercoiling (23,24,26,28,29). The helicase domain of reverse gyrase carries all determinants for ATP binding and hydrolysis (29). Its architecture is reminiscent of the helicase core of DEAD-box RNA helicases (13,25,27,62), and it carries the conserved signature motifs of this helicase family (43,63) (reviewed in (64)). Despite pronounced deviations of these motifs from the consensus sequence (43), ATP binding involves similar residues and interactions as in DEAD-box proteins (27) (see 'structure' section; Figure 1E). Mutations of the conserved motifs in *Tma*_rgyr abolish ATP binding and/or hydrolysis and DNA supercoiling (30,31), highlighting the central role of the helicase module for reverse gyrase function.

DEAD-box proteins undergo a cycle of nucleotide-dependent conformational changes that is the basis for their ATP-dependent stabilization of RNA duplexes (reviewed in (58)). The conformational states of the isolated *Tma*_rgyr helicase domain during the nucleotide cycle have been delineated in single molecule FRET experiments (23,26), using the ATP analogs 5'-adenylyl-β,γ-imidotriphosphate (ADPNP) (to mimic an initial collision complex), ADP·BeF_x (to mimic the pre-hydrolysis state, formed from the initial collision complex by isomerization) and ADP·MgF_x (to mimic a state after ATP hydrolysis, but before phosphate release), as well as ADP (to populate the state after phosphate release; Figure 2). The conformational cycle has been characterized in the presence of different DNAs, and the affinities of each nucleotide state for these DNA substrates have been determined (23,26,29) (Figure 2). ATP and DNA bind with a positive thermodynamic linkage to the helicase domain (29), and induce a closing of the cleft between H1 and H2 (26). The conformational change explains the DNA-stimulated ATPase activity of the helicase domain and of reverse gyrase (30). The increase in the turnover number k_{cat} depends on the type of the DNA bound, and ranges from 40–50-fold for linear ss- or dsDNA, to 22-fold for plasmid DNA and 10-fold for a

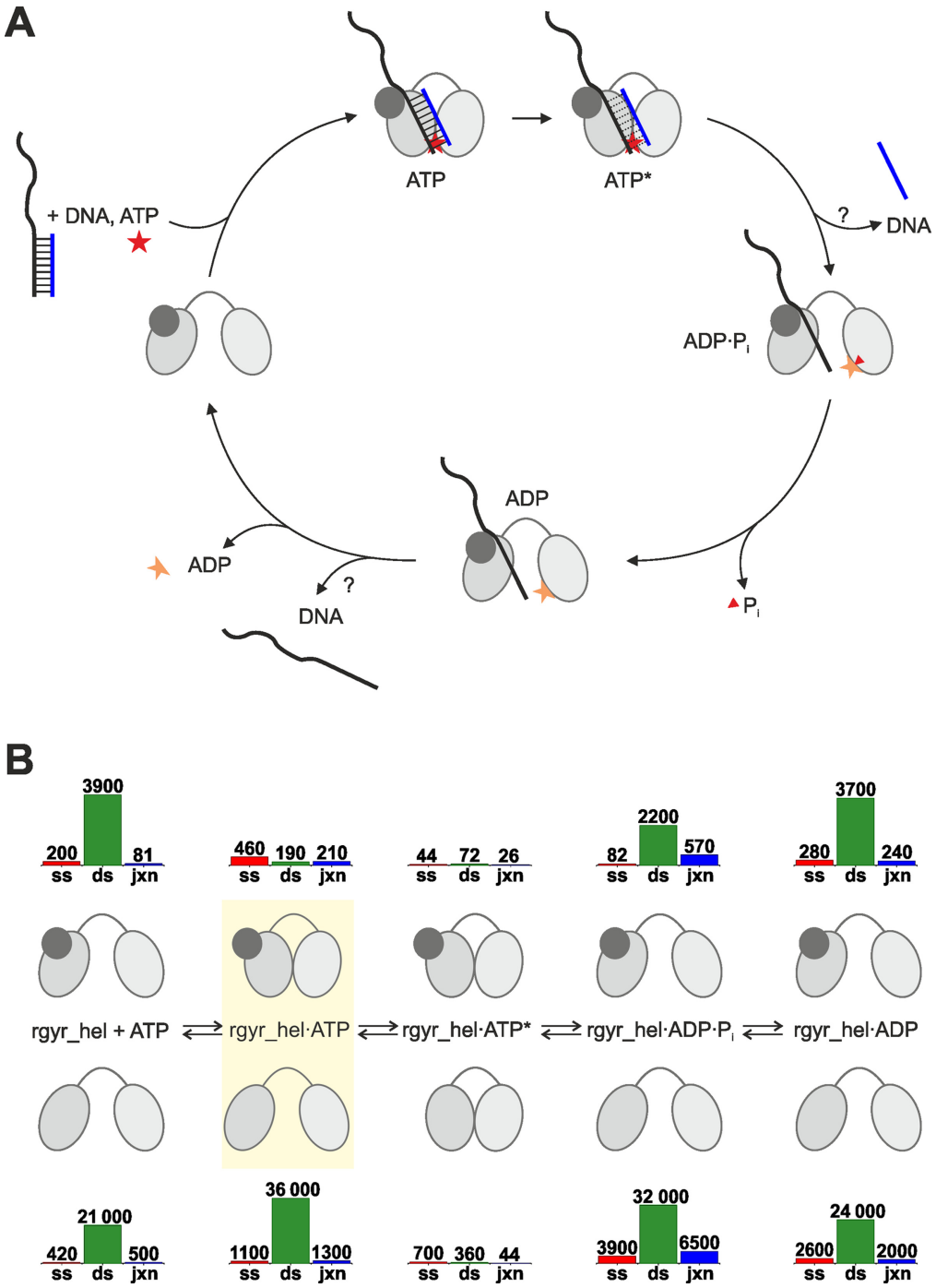

Figure 2. Conformational changes of the helicase domain are linked to DNA affinity. (**A**) Conformational cycle of the reverse gyrase helicase domain. The different conformations of the *Tma*_rgyr helicase domain at each state of the nucleotide cycle were delineated using the isolated helicase domain with a donor and acceptor fluorophore on opposite sides of the cleft between H1 and H2, and ADPNP, ADP·BeF_x, ADP·MgF_x and ADP as nucleotide (analog)s. The helicase core alternates between open and closed states. Closing is triggered by cooperative binding of DNA and ATP, and re-opening occurs upon ATP hydrolysis. The star denotes an isomerized ATP-bound state, mimicked by ADP·BeF_x. The dotted lines for the base pairs indicate the local destabilization of the duplex in this state. The helicase module of *Tma*_rgyr can transiently unwind a short DNA duplex in an ATP-dependent reaction (24). The catalytic cycle of unwinding is shown in analogy to DEAD-box proteins. Light gray oval: H1, gray oval: H2, dark gray (small) oval: latch, orange star: ATP, red triangle: P_i. DNA is depicted schematically. (**B**) Affinities of the isolated *Tma*_rgyr helicase domain for different DNA substrates throughout the nucleotide cycle. The bars represent the K_d values of the respective DNA complexes, and are thus inversely related to the affinity. K_d values are given in nM. K_d values listed for the ADP·P_i state of the helicase domain are DNA affinities determined in the presence of ADP·MgF_x. ADP·MgF_x is not a product state analog, but mimics a nucleotide state after ATP hydrolysis, but before phosphate release (post-hydrolysis state). ss: ssDNA (red), ds: dsDNA (green), jxn: ss/dsDNA junction (blue). The upper panel shows conformation and DNA affinities for the helicase domain including the latch. The bottom panel shows the conformation and DNA affinities for the helicase domain lacking the latch. Light gray oval: H1, gray oval: H2, dark gray (small) oval: latch. The different conformation of the two variants in the ATP-state is highlighted in yellow. The conformational switch of the helicase domain is coupled to a switch in dsDNA affinity.

short 9/14mer DNA (24,29). In the context of reverse gyrase, the DNA-stimulation is about 10-fold less, suggesting a repression of the ATPase activity by the topoisomerase domain (29,30). The cleft in the helicase core remains closed during a subsequent isomerization step. Re-opening of the cleft occurs upon ATP hydrolysis, the rate-limiting step in the nucleotide cycle (at least in the absence of DNA) (26,30), and thus before phosphate and ADP release. Overall, the helicase domain of reverse gyrase thus undergoes a similar conformational cycle as DEAD-box proteins (65–67) (reviewed in (58)), alternating between open and closed states with different DNA affinities (Figure 2B). While closing is coupled to the cooperative binding of ATP and DNA/RNA in reverse gyrase and DEAD-box proteins alike, reopening occurs at different steps: with ATP hydrolysis for the reverse gyrase helicase domain (26), and with the rate-limiting step of phosphate release in DEAD-box proteins (65,68). The conformational change of the reverse gyrase helicase domain is coupled to a switch in dsDNA affinity, with a low affinity in the open state, and a high affinity in the closed state. In contrast to dsDNA, the switch to high affinity for ssDNA occurs after cleft closure, concomitant with the isomerization step, and the return to low ssDNA affinity occurs after re-opening of the cleft, with phosphate release (Figure 2B). This uncoupling of the conformational switch and the switch in ssDNA affinity points to contributions of the non-canonical insertions in the helicase core, namely the latch and/or the insert helix, to ssDNA binding (see below).

Overall, these data are in agreement with the general principle of the proposed affinity-switch-model (61). However, the picture is clearly more complex than a mere alternation between ATP and ADP states with high dsDNA and ssDNA affinities. Comparison of the affinities of the individual nucleotide states for ssDNA, dsDNA and a ss/dsDNA junction (23,26,29) (Figure 2B) allows for further dissection of DNA binding by the helicase domain throughout the catalytic cycle. In the nucleotide-free state, the helicase domain shows a higher affinity for an ss/dsDNA junction than for either ssDNA or dsDNA, indicating that the helicase domain directly binds to the junction (26). Although the nucleotide-free state is probably not populated in steady-state equilibrium in the cell due to the high concentration of nucleotides, it is an obligate intermediate during ADP-to-ATP exchange, and may serve to anchor reverse gyrase on ss/dsDNA junctions from one catalytic cycle to the next. The ss/dsDNA junction is most strongly bound in the ADP·BeF_x-mimicked pre-hydrolysis state, a state that also binds ssDNA and dsDNA with equally high affinity. In the ADP·MgF_x and ADP states, the affinity for the junction resembles the affinities for ssDNA, suggesting that the ssDNA region is mainly contacted at the end of the catalytic cycle. Thereby, the helicase domain may sense if there are still single-stranded regions in the DNA substrate that need to be re-wound, or if the single-stranded regions have disappeared, and reverse gyrase has fulfilled its task.

ATP and DNA binding and DNA-stimulated ATPase = ATP-dependent DNA unwinding?

In DEAD-box proteins, the transition to the closed conformation has been linked to destabilization of a bound duplex (62). Based on the energetic difference of 12 kJ/mol between the collision complex (bound to ADPNP and dsDNA, closed conformation) and the isomerized state of the helicase domain (bound to a ADP·BeF_x and a ss/dsDNA junction, closed conformation) we predicted that this step may be coupled to the disruption of 2–3 bp (26). In the isomerized state, the helicase domain does not show a preference for ssDNA versus dsDNA or ss/dsDNA junctions (26), which may point to facilitated inter-conversion of ssDNA and dsDNA. Indeed, unwinding of a short DNA duplex was detected when the helicase domain or reverse gyrase were trapped in the ADP·BeF_x-bound state (24), showing that reverse gyrase is capable of transient ATP-dependent duplex separation. The inserts in the helicase core, the latch and the insert helix, contribute to duplex unwinding by the helicase domain (24). The helicase domain of reverse gyrase thus stabilizes or expands single-stranded regions that are already present in DNA at high temperatures, or might even create single-stranded regions *de novo* by its local unwinding activity.

Insertions into the canonical helicase core modulate DNA binding and unwinding, and affect DNA supercoiling

The latch is required for thermodynamic coupling of DNA and ATP binding, for duplex unwinding and DNA supercoiling. Despite its low level of sequence conservation and structural diversity, deletion of the latch leads to a complete loss of cooperativity of nucleotide and DNA binding in *Tma*_rgyr (28), and DNA affinity is reduced in all nucleotide states (23). Deletion of the latch also abolishes DNA unwinding (24) and supercoiling by reverse gyrase (28). From the complete characterization of helicase core conformations and DNA affinities of all nucleotide states for a helicase domain lacking the latch (23,26,28), the contributions of the latch at individual stages of the nucleotide cycle have become evident (Figure 2B). In the *Tma*_rgyr helicase domain lacking the latch, the positive thermodynamic coupling of ATP and DNA binding is lost (28). As a consequence, the energetic differences between the collision complex and the isomerized complex are reduced, and the enzyme fails to unwind duplex DNA (24). In the absence of the latch, the transition to the closed conformation and the concurrent increase in DNA affinity is shifted to the ADP·BeF_x-state (23). This pre-hydrolysis state is still the nucleotide-state with the highest DNA affinity, although the affinities are generally reduced in the absence of the latch. The ssDNA affinity of the pre-hydrolysis state is most severely decreased (16-fold, corresponding to 7 kJ/mol at 298 K). As a consequence, the helicase domain lacking the latch now shows a strong preference for an ss/dsDNA junction (23). It still preferentially binds ssDNA after ATP hydrolysis, in the ADP·MgF_x state, but the ssDNA affinity is even more severely reduced (48-fold, 10 kJ/mol) compared to the helicase domain with the latch (23). The latch thus contributes to DNA binding only transiently, before and after ATP hydrolysis. The loss in ssDNA affinity toward the end of the catalytic cycle may further explain the lack of unwinding activity of *Tma*_rgyr lacking the latch because single-stranded regions are no longer stabilized (23).

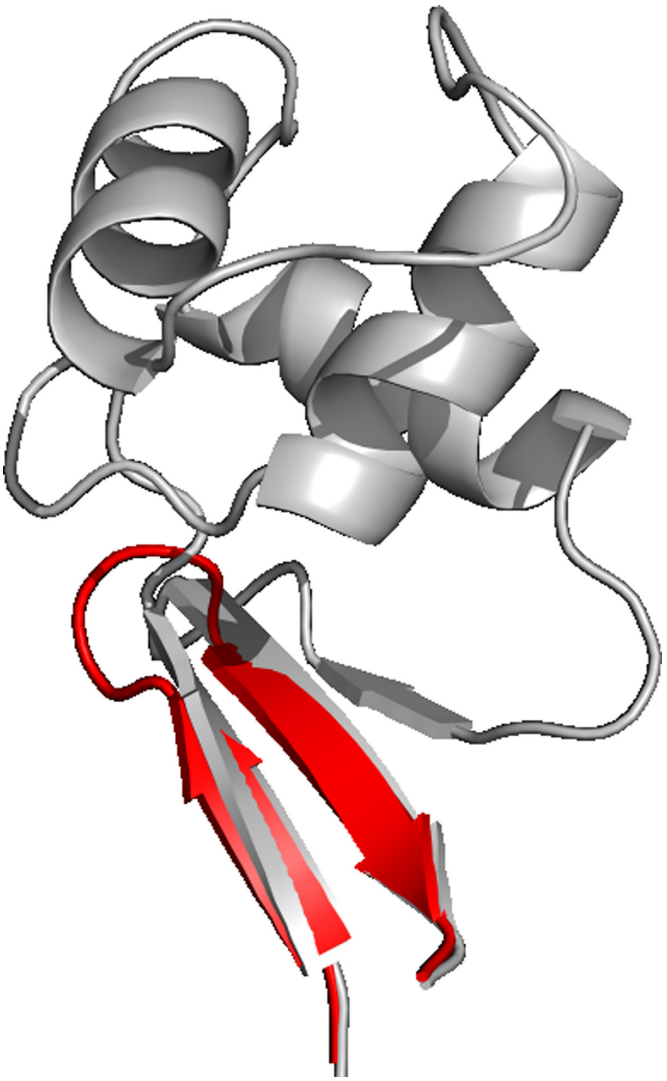

Figure 3. Structure of the latch in different reverse gyrases. Superposition of the *Tma*_rgyr latch (gray) and a homology model of the *Taf*_rgyr latch (red). The homology model of *Taf*_rgyr was generated with Protein Homology/analogY Recognition Engine V 2.0 'Phyre2' (69) using *Tma*_rgyr (PDB ID: 4ddv) as a template. All residues were modeled at >90% confidence. Deletion constructs of *Afu*_rgyr lacking the latch have retained the β-hairpin present in *Taf*_rgyr. The resulting variant still shows positive DNA supercoiling activity. In contrast, the β-hairpin is not present in *Tma*_rgyr and *Tte*_rgyr variants lacking the latch that lost their positive DNA supercoiling activity. Possibly, the β-hairpin constitutes a minimal functional latch.

A role of the latch in communication between the helicase and topoisomerase domains in reverse gyrase has been put forward (13). However, effects of the latch in *Afu*_rgyr (14,15), *Tma*_rgyr (23,24,28) and *Tte*_rgyr (19) are not entirely consistent and difficult to reconcile. While *Afu*_rgyr lacking the latch is still capable of positive DNA supercoiling (15), *Tte*_rgyr (19) and *Tma*_rgyr (28) lose their supercoiling activity upon latch deletion. Notably, the different variants were generated by deleting different parts of the latch (Figure 3). For *Tte*_rgyr (19) and *Tma*_rgyr (28) the full latch was deleted, including the two short β-strands that form the β-sheet connecting the latch to H2 (Figure 3). The *Afu*_rgyr variant lacking the latch still contained this β-sheet. Interestingly, *Taf*_rgyr contains a very small latch (amino acids 385–395) with sequence homology to these β-strands, that is modeled (using Protein Homology/analogY Recognition Engine V 2.0 (Phyre2) (69) and *Tma*_rgyr (PDB ID: 4ddv) as a template) with high confidence as a β-hairpin protruding from H2 (Figure 3). It is tempting to speculate that this minimal motif might be sufficient for inter-domain communication and positive DNA supercoiling. It is unclear at the moment if the latch undergoes relative movement to H2 during the catalytic cycle. Increased nucleotide affinities (in *Tma*_rgyr (23,28)) and ATPase activities (*Afu*_rgyr (15)) upon latch deletion have been interpreted as an indication that part of the energy of ATP binding and/or hydrolysis may be converted into a displacement of the latch (15).

The H1 insertion contributes to DNA binding, ATP hydrolysis and DNA unwinding. Similar to the latch, the H1 insertion shows great variability in sequence and length (25) (Supplementary Figure S1). It appears to be completely missing in *Aciduliprofundum boonei* reverse gyrase, and reaches a length of 84 amino acids in the *Hyperthermus butylicus* enzyme. In *Afu*_rgyr, this region folds into a β-hairpin (amino acids 201–217) that protrudes from H1 on the same face of reverse gyrase as the latch (13). The orientation is similar in *Tma*_rgyr, but here the insert forms a larger loop-helix structure (amino acids 224–249) (25). Its deletion moderately reduces DNA affinity (24,25). The intrinsic ATPase activity is lost, and the DNA-stimulated ATPase activity is reduced 2-fold (24,25). The insert is distant from the nucleotide binding site in H1 and H2 (13,25), and its effect on the nucleotide cycle of the helicase domain is most likely indirect (24). Deletion of the insert also leads to a 2–10-fold reduction in the rate of duplex unwinding by the *Tma*_rgyr helicase domain (depending on the polaritiy of the single-stranded overhang) (24). *Tte*_rgyr lacking the insert also shows slightly reduced DNA affinity, and is ATPase- and supercoiling-deficient, but is still capable of relaxing DNA (19). Similar to the latch, the functional implications of this insert thus appear to be context-dependent, and may vary between different reverse gyrases.

The zinc fingers

The zinc fingers were originally suggested to contribute to DNA binding and to guide strand passage (13). Mutational studies confirmed a contribution to DNA binding, albeit with different results for different enzymes. It has to be noted that two (19,31) out of the three studies that addressed the role of the zinc fingers were performed in the absence of zinc, possibly affecting the stability of the zinc fingers and the overall enzyme. In the context of the isolated *Tma*_rygr helicase domain, the presence of Zn1 interferes with ssDNA and dsDNA binding, suggesting a detrimental effect of Zn1 on DNA-binding in the absence of the topoisomerase domain (25). In the ADPNP-bound state the effect on dsDNA is larger, while in the ADP-bound state ssDNA binding is more affected. Zn1 deletion also increases the DNA-stimulated ATPase activity of the helicase domain, and reduces the apparent K_M value for DNA, $K_{M,app,DNA}$

(more for dsDNA than for ssDNA) (25). $K_{M,app,DNA}$ is a measure for the DNA affinity of the nucleotide state populated under steady-state conditions. For ATP hydrolysis as the rate-limiting step in the catalytic cycle, this would be the ADP·P_i state. Altogether, it thus seems that the contribution of Zn1 to DNA binding depends on the nucleotide state of the helicase domain. Mutation of Zn1 in *Tma*_rgyr leads to a loss in affinity for ssDNA, has little effect on the ATPase activity, and reduces the positive supercoiling activity (31). Deletion or mutation of Zn1 and Zn2 abolishes supercoiling and DNA relaxation activities of *Tma*_rgyr (25), possibly pointing toward a contribution to strand passage. Structurally, the two zinc fingers are ideally positioned at the end of the cleavage site, and might either contact ssDNA adjacent to the cleavage site, or contact the double-stranded region further away from the bubble (25). Individual deletion of Zn1 and Zn2 in *Tte*_rgyr significantly impairs binding to an ss/dsDNA junction, and slightly reduces the ATPase activity (19). The supercoiling activity is lost, but the enzyme can still relax DNA. From the currently available data, no clear picture for the general role of the zinc fingers in reverse gyrases is emerging.

'Model refinement': coupling of ATP-dependent conformational changes to DNA processing during positive supercoiling

Reverse gyrase is able to introduce positive supercoils into DNA, but relaxes DNA in the absence of the latch (or in the presence of other nucleotides than ATP). Supercoiling and relaxation are commonly explained as the result of strand passage in opposite directions. It should be noted that relaxation of negatively supercoiled DNA and positive supercoiling of relaxed DNA both increase the linking number of the DNA, and are a consequence of strand passage in the same direction. The energetic requirements for both reactions are different, however: relaxation is an energetically favorable reaction, and can be driven by the torsional energy of the DNA. In contrast, positive supercoiling is energetically unfavorable, and therefore requires coupling to ATP hydrolysis. In the presence of ATP, reverse gyrase catalyzes positive DNA supercoiling, and thus mediates strand passage selectively toward an increase in linking number (2). The picture is different for topoisomerase IA that can catalyze the relaxation of negative or positive supercoils (70): relaxation of negatively supercoiled DNA is associated with an increase in linking number, whereas relaxation of positively supercoiled DNA corresponds to a decrease in linking number. Topoisomerase IA thus catalyzes strand passages in both directions. Here, both reactions are energetically favorable. The direction of strand passage is determined by the torsional energy of the DNA, and leads to relaxation.

How can strand passage in opposite directions be envisaged in an enzyme/DNA complex, with the DNA bound in a defined geometry? A strikingly simple conceptual model involves the formation of a loop by the non-cleaved strand of the DNA (Figure 4A) in the gap that has been created by cleavage of the other DNA strand. If the loop is stabilized in a left-handed configuration, religation of the cleaved strand 'through' the loop will eventually remove a helical turn, and thus lead to a reduction of the linking number by $\Delta lk = -1$ (Figure 4A and B). This reaction sequence corresponds to the relaxation of positively supercoiled DNA (and formally to the ATP-dependent negative supercoiling of relaxed DNA, although not catalyzed by type I topoisomerases). Stabilization of the loop in a right-handed configuration and religation 'through' the loop, on the other hand, will add a helical turn, and therefore increase the linking number by $\Delta lk = +1$ (Figure 4A and B). This reaction sequence represents the relaxation of negatively supercoiled DNA, or the ATP-dependent introduction of positive supercoils. Although there is currently no experimental evidence for formation of a single-stranded loop in DNA bound to reverse gyrase, loop formation could be envisaged as a consequence of DNA cleavage and possibly by conformational changes of the topoisomerase IA module. In topoisomerase IA, the geometry of the loop would be determined by the supercoiling state of the DNA substrate: the torsional energy of negatively supercoiled DNA would favor the right-handed configuration, followed by strand passage toward an increase in the linking number and relaxation. In contrast, the torsional energy of positively supercoiled DNA would favor the left-handed configuration, and strand passage toward a decrease in the linking number also leads to relaxation.

Reverse gyrase could bias strand passage toward an increase in linking number either directly by stabilizing a right-handed configuration of the loop, and/or indirectly by preventing formation of the left-handed loop. As a topoisomerase IA module can in principle catalyze bidirectional strand passage, a prevention of the DNA conformation leading to a decrease in linking number by reverse gyrase appears more likely. This selective effect is most likely brought about by the helicase module, the distinctive element of reverse gyrase. The conformational cycle of the helicase module is linked to switches in dsDNA affinity, implying that a binding site for dsDNA is created upon closure of the cleft between H1 and H2. Binding of the helicase core to the duplex adjacent to the bubble will alter the angle between the two ends of the bound DNA region, and might impose a structural change on the non-cleaved single strand, disfavoring a left-handed loop and/or favoring a right-handed loop. It should be noted that binding of reverse gyrase to the duplex regions flanking the bubble could also rationalize a segregation of underwound and overwound regions by the enzyme, as postulated in the domain model (71) (see above). The underwound region would be generated by strand separation and bubble formation, either spontaneously at high temperatures, or assisted by the helicase activity of reverse gyrase. In a topologically constrained circular DNA, the formation of an underwound region would be compensated by the formation of overwound regions in the remainder of the DNA. Positive supercoiling would then be the result of selective relaxation of a negative supercoil. As discussed above, relaxation of negative supercoils is also associated with strand passage toward an increase in linking number. From a mechanistic perspective, the domain model and the controlled strand passage model, i.e. biasing strand passage toward an increase in linking number, are thus equivalent and not mutually exclusive.

Altogether, this brings us to the following possible model for positive supercoiling of DNA by reverse gyrase: At the

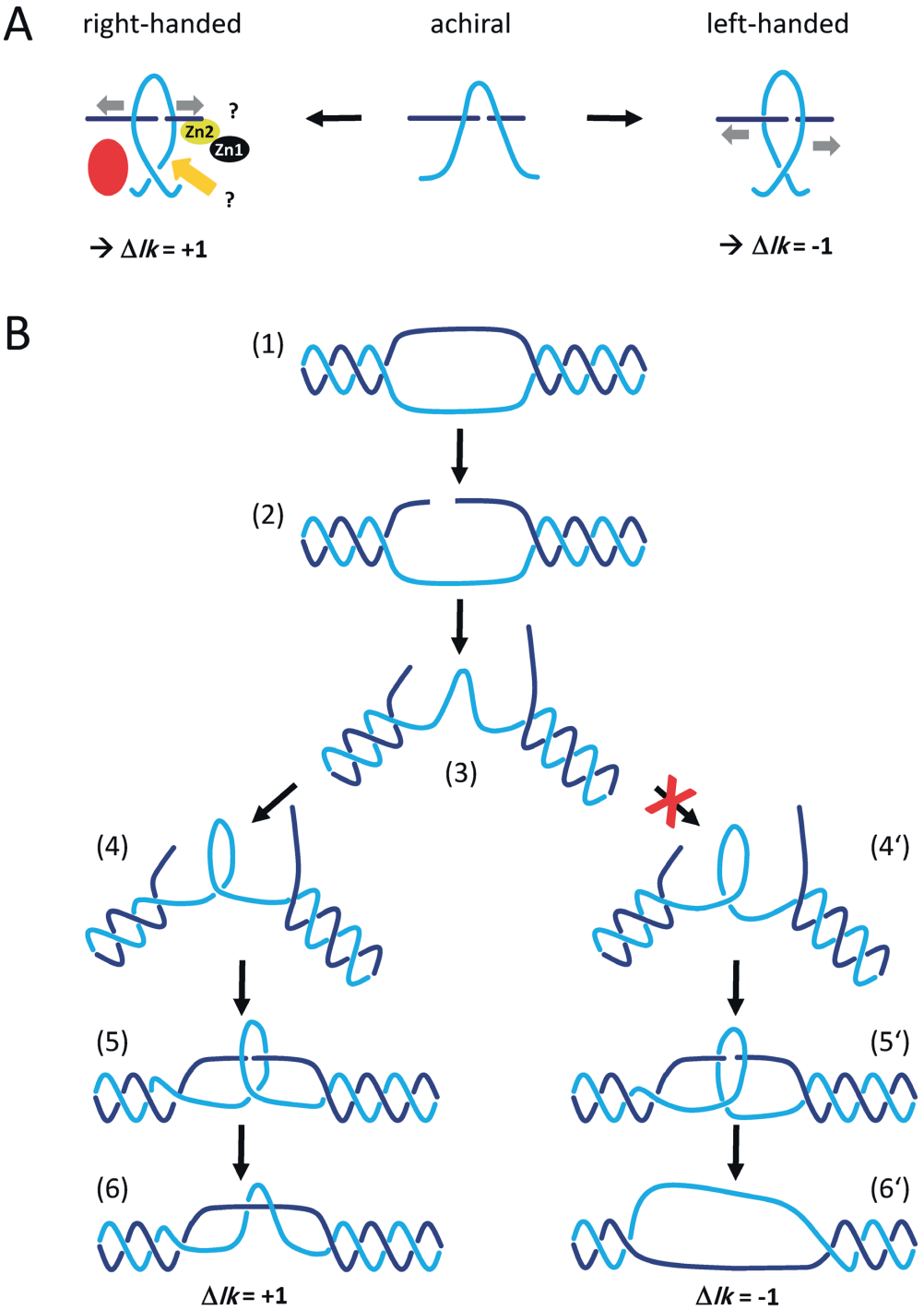

Figure 4. Biasing 'strand passage' toward positive supercoiling: a model. (**A**) Principle. The model shows a cleaved DNA strand (dark blue) and a non-cleaved DNA strand (blue) that passes through the gap (center panel: achiral loop). Stabilization of this loop in a left-handed geometry (right panel) and religation of the first strand 'through' the loop will result in the loss of one crossing of the strands, and thus to a decrease in linking number of the DNA ($\Delta lk = -1$). Stabilization of a right-handed loop (left panel) and religation, in contrast, introduces one crossing into the DNA, and increases its linking number ($\Delta lk = +1$). Reverse gyrase may bias strand passage toward increased linking numbers and positive supercoiling of DNA by stabilizing the right-handed configuration, involving the latch (red), the insert in H1 (orange arrow) and possibly Zn1 and Zn2 (black, yellow). The gray arrows indicate the direction of movement for the two flanks of the achiral loop to generate the right-handed or left-handed crossing. (**B**) Step-by-step depiction of the increase in linking number and positive DNA supercoiling versus decreases in the linking number. The scissile DNA strand (dark blue) of a DNA bubble (1) is cleaved (2). A reorientation of the DNA creates a gap between the ends of the cleaved strand, and distorts the non-cleaved strand (blue) into a loop (3). This loop can be stabilized in a right-handed (4) or left-handed crossing (4′). A reversal of the DNA orientation (from 2 to 3) will bring the ends of the cleaved strand together (5, 5′), and religation will fix the created crossing (6, 6′). For the right-handed loop (4), religation will lead to an increase of the linking number ($\Delta lk = +1$), for the left-handed loop (4′), the linking number will decrease ($\Delta lk = -1$). Strand passage can be biased toward an increase in linking number and positive supercoiling by interfering with stabilization of the left-handed loop (red cross), and/or by stabilizing the right-handed crossing.

beginning of the catalytic cycle, reverse gyrase binds to an internal single-stranded DNA bubble (Figure 5, state 1), generated by spontaneous strand separation at high temperatures, or by the helicase activity of reverse gyrase. The latch and the H1 insert help stabilize the bubble, and one of the DNA strands is cleaved (Figure 5, state 1). ATP binding to the helicase core will then lead to closure of the cleft between H1 and H2 (Figure 5, states 2, 2′). The conformational change generates a dsDNA binding site, and the helicase core can now interact with duplex DNA flanking the bubble on either side (Figure 5, states 2, 2′). The fixation of the adjacent duplex regions might separate the underwound DNA bound by the enzyme from compensating positive supercoils in other parts of the DNA. At the same time, the conformational change of the helicase core will alter the geometry of the bound bubble, and affect the relative arrangement of helicase and topoisomerase domains. H1 is connected to the TOPRIM domain by an extensive interface, whereas the interaction surface of H2 and the latch with the topoisomerase module is less extensive. During closure of the cleft, H1 thus most likely remains connected to the topoisomerase module. The movement of H2 toward H1 will result in the displacement of the latch, and will open the interface between latch and lid. The postulated large-scale movement of the lid, an up-swinging upon closure of the helicase domain and latch release, has not been observed for any type IA topoisomerase. From a structural perspective a more subtle swiveling of the lid is also possible, and perhaps more likely. It is conceivable that the concerted movements in the reverse gyrase/DNA complex upon ATP binding create tension in the non-cleaved strand of the DNA bubble, leading to formation of a single-stranded loop within the gap between the ends of the cleaved strands, a process that may be facilitated by opening of the lid (Figure 5, state 2, 2′). At this stage, and particularly once the bound ATP has been hydrolyzed, the latch tightly interacts with ssDNA, and thus possibly stabilizes the conformation of the single-stranded DNA (Figure 5, state 3). The tighter ssDNA binding may be facilitated by the release of the duplex DNA with reopening of the helicase core when ATP has been hydrolyzed. It is not clear if the latch contacts the scissile/cleaved or the non-cleaved DNA strand. The latch is not required for strand cleavage, strand passage and religation *per se*, as evident from the relaxation activity of reverse gyrase lacking the latch. Instead, its predominant role appears to be in determining the direction of strand passage. Such a bias of the direction of strand passage toward positive supercoiling can be brought about in two different ways: either the latch actively promotes strand passage toward an increase in linking number and eventually positive supercoiling, e.g. by a joint movement with the bound ssDNA in the required direction, or it acts as an inhibitory element and impedes strand passage toward decreasing linking numbers, which would be the energetically favored reaction. Given the structural diversity of the latch, it seems likely that the latch rather acts as a passive element that helps stabilize the DNA in the correct geometry to drive strand passage toward positive supercoiling (Figure 5, state 3). The helical insert and possibly the zinc fingers might contribute to this selection. The stabilization of the loop by the latch would imply that the latch adopts a different orientation with respect to H2 before (Figure 5, state 2, 2′) and after ATP hydrolysis (Figure 5, state 3), in agreement with its increased contribution to ssDNA binding in the post-hydrolysis state. The right-handed geometry of the loop would have the correct chirality, such that religation leads to an increase in linking number, and the introduction of a positive supercoil (Figure 5, states 3, 4). Religation requires a reversal of the movement of the lid, which should be accompanied by resetting of the latch to its resting position (Figure 5, state 4). The trigger for this movement is currently unclear, although release of the latch from the DNA could be linked to its reduced affinity for the rewound DNA. At the end of the catalytic cycle, the linking number of the DNA has increased by $\Delta lk = +1$. Overall, this model links the conformational cycle of the helicase module with binding of reverse gyrase to DNA bubbles, and assigns dedicated roles to the latch, the H1 insert, and possibly the zinc fingers in imposing a DNA geometry that leads to unidirectional strand passage and positive DNA supercoiling. DNA processing by reverse gyrase according to this model is thus not a sequential event, with the helicase domain unwinding DNA in a first step, and then handing the DNA over to the topoisomerase domain for strand passage and supercoiling, but is the result of an intricate cooperation of both domains at all stages of the reaction.

OPEN QUESTIONS: CONCLUSIONS AND OUTLOOK

Although a more refined picture of the mechanism of positive supercoiling has emerged from the extensive studies in the past years, the reverse gyrase mystery has not entirely been solved yet. A mechanistic understanding of the positive supercoiling reaction at a molecular level requires the identification of the intermediates of the catalytic cycle, and knowledge on the rate constants of individual steps. While the nucleotide-dependent conformational cycle of the isolated helicase domain has been delineated, the conformational changes of the topoisomerase domain, such as the movement of the lid to generate a gap in the cleaved DNA strand and reversal of this movement as a prerequisite for religation, are still elusive. Future studies will have to address conformational changes of the helicase and the topoisomerase domain in the context of reverse gyrase, including movements of the latch and the H1 insert, and the latch in relation to the lid. A movement of the latch relative to H2, inferred from changes in its contribution to ssDNA affinity, has not been demonstrated experimentally. It is also unclear which of the two DNA strands in the bubble is contacted by the latch. The functional role of the zinc fingers remains enigmatic. Although they are clearly critical for the overall reaction, their specific effects on individual steps have been difficult to pinpoint. The proposed function of the zinc fingers in guiding strand passage has not been proven, and it is equally possible that they predominantly serve a structural role by providing a rigid platform for the conformational changes that occur during catalysis. Future studies will have to address possible contributions of the zinc fingers to DNA binding at each stage of the nucleotide cycle, and their movements, if any, during the DNA supercoiling reaction.

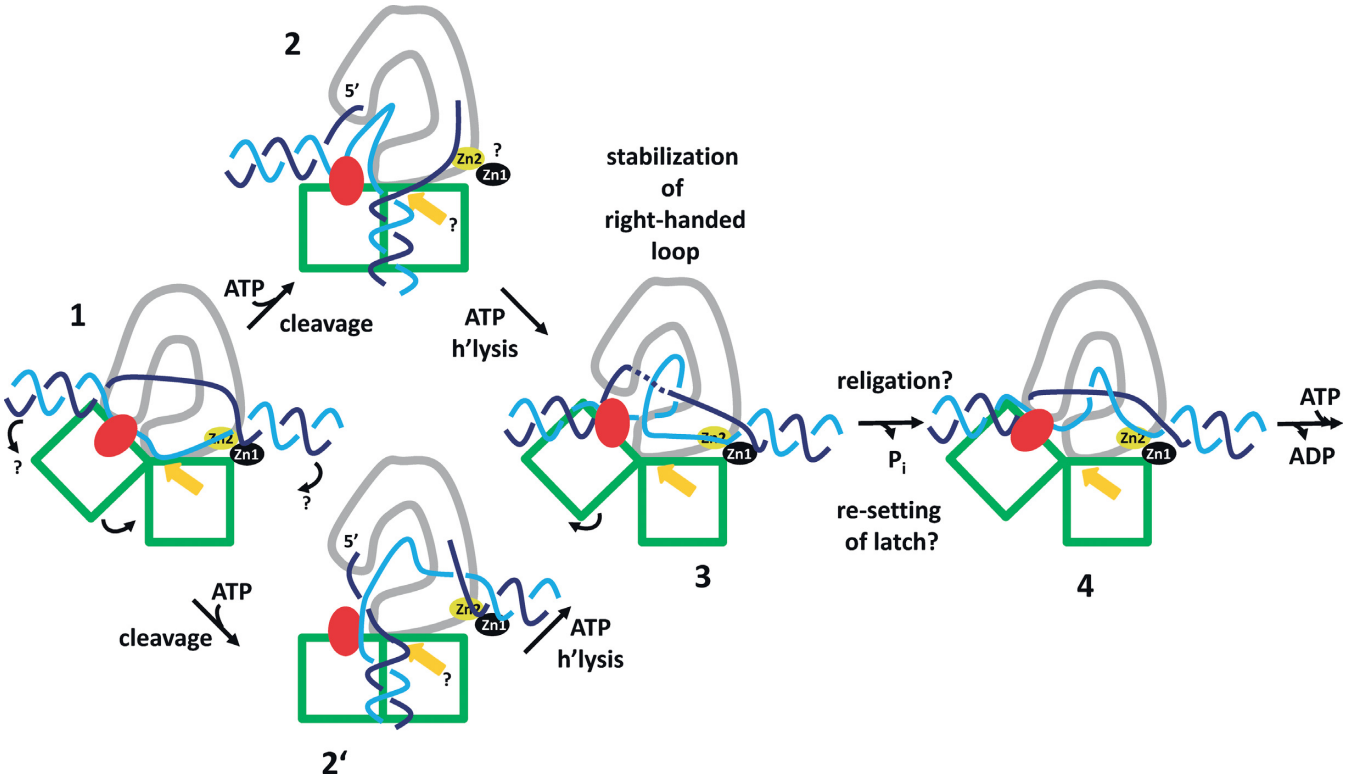

Figure 5. Refined mechanistic model for positive supercoiling of DNA by reverse gyrase. The catalytic cycle of reverse gyrase starts with binding of the enzyme to a single-stranded bubble (1; scissile strand: dark blue, non-cleaved strand: blue).The helicase domain (green squares) is in the open conformation, with an open cleft between H1 and H2. The latch (red) and the insert in H1 (orange) contact single-stranded regions and help stabilize the bubble. Gray: topoisomerase domain. DNA cleavage can occur in the absence of ATP. Upon ATP binding, the cleft between H1 and H2 will close (2, 2′). Movement of H2 toward H1 will disengage the latch from the lid, and the lid undergoes an upward or a more subtle sideways or rotational movement. As a consequence, the distance between the 5′-end of the cleaved DNA strand, covalently attached to the catalytic tyrosine, and the 3′-end, possibly bound in an ssDNA binding groove, will increase. The conformational change of the helicase domain generates a high affinity binding site for dsDNA, and the helicase domain will bind one of the duplex regions flanking the bubble (2: binding to the left end, 2′: binding to the right end). Binding the duplex region will alter the geometry of the bound duplex, and help deform the non-cleaved strand into a loop ('strand passage'). In a next step, ATP hydrolysis leads to re-opening of the helicase core. The latch remains tightly bound to ssDNA and adopts a different relative orientation to H2 than before hydrolysis. In this configuration it causes a deformation of the loop into a positive, right-handed crossing (3), possibly together with the insert and Zn1 and Zn2. Religation requires reversal of the movement of the lid, and fixes a positive crossing (4). The latch may be released and resume its original position because of its reduced affinity for the rewound DNA, and will reengage in interactions with the lid. Exchange of ADP for ATP then starts the next catalytic cycle.

It is also still unclear how the movements in the helicase domain, of the non-canonical insertions, and of the topoisomerase domain are orchestrated at the molecular level. What are the triggering events for individual conformational changes? As a first step toward understanding the dynamics of the reverse gyrase/DNA complex during catalysis, it will be important to identify the elements of reverse gyrase that contact specific regions of the bound DNA at each step of the nucleotide cycle. In addition to conformational changes of the enzyme, the conformational changes of the bound DNA substrate during a catalytic cycle will have to be addressed. Understanding the spatio-temporal regulation of conformational changes in the reverse gyrase/DNA complex is the key to understand the mechanism of positive DNA supercoiling. Ultimately, a mechanistic understanding of positive DNA supercoiling may also help uncover the physiological function of reverse gyrase and the role of its hallmark reaction in the physiological context. Functional cooperation of helicases and topoisomerases is a wide-spread motif in the maintenance of genome stability in all kingdoms of life, and reverse gyrase may be a valuable model to further our understanding of the principles underlying their joint cellular function.

SUPPLEMENTARY DATA

Supplementary Data are available at NAR Online.

ACKNOWLEDGMENT

We thank Markus Rudolph and Airat Gubaev for constructive discussions and previous and current lab members for their contributions.

ACCESION NUMBERS

PDB IDs: 4ddu and 4ddv.

FUNDING

Swiss National Science Foundation and the Deutsche Forschungsgemeinschaft [SFB 858]. Funding for open access charge: Deutsche Forschungsgemeinschaft.

Conflict of interest statement. None declared.

REFERENCES

1. Kikuchi,A. and Asai,K. (1984) Reverse gyrase–a topoisomerase which introduces positive superhelical turns into DNA. *Nature*, **309**, 677–681.
2. Forterre,P., Mirambeau,G., Jaxel,C., Nadal,M. and Duguet,M. (1985) High positive supercoiling in vitro catalyzed by an ATP and polyethylene glycol-stimulated topoisomerase from *Sulfolobus acidocaldarius*. *EMBO J.*, **4**, 2123–2128.
3. Nakasu,S. and Kikuchi,A. (1985) Reverse gyrase; ATP-dependent type I topoisomerase from *Sulfolobus*. *EMBO J.*, **4**, 2705–2710.
4. Nadal,M., Jaxel,C., Portemer,C., Forterre,P., Mirambeau,G. and Duguet,M. (1988) Reverse gyrase of *Sulfolobus*: purification to homogeneity and characterization. *Biochemistry*, **27**, 9102–9108.
5. Gellert,M., Mizuuchi,K., O'Dea,M.H. and Nash,H.A. (1976) DNA gyrase: an enzyme that introduces superhelical turns into DNA. *Proc. Natl. Acad. Sci. U.S.A.*, **73**, 3872–3876.
6. Jaxel,C., Bouthier de la Tour,C., Duguet,M. and Nadal,M. (1996) Reverse gyrase gene from *Sulfolobus shibatae* B12: gene structure, transcription unit and comparative sequence analysis of the two domains. *Nucleic Acids Res.*, **24**, 4668–4675.
7. Jaxel,C., Duguet,M. and Nadal,M. (1999) Analysis of DNA cleavage by reverse gyrase from Sulfolobus shibatae B12. *Eur. J. Biochem.*, **260**, 103–111.
8. Bizard,A., Garnier,F. and Nadal,M. (2011) TopR2, the second reverse gyrase of Sulfolobus solfataricus, exhibits unusual properties. *J. Mol. Biol.*, **408**, 839–849.
9. Borges,K.M., Bergerat,A., Bogert,A.M., DiRuggiero,J., Forterre,P. and Robb,F.T. (1997) Characterization of the reverse gyrase from the hyperthermophilic archaeon Pyrococcus furiosus. *J. Bacteriol.*, **179**, 1721–1726.
10. Kozyavkin,S.A., Krah,R., Gellert,M., Stetter,K.O., Lake,J.A. and Slesarev,A.I. (1994) A reverse gyrase with an unusual structure. A type I DNA topoisomerase from the hyperthermophile *Methanopyrus kandleri* is a two-subunit protein. *J. Biol. Chem.*, **269**, 11081–11089.
11. Krah,R., Kozyavkin,S.A., Slesarev,A.I. and Gellert,M. (1996) A two-subunit type I DNA topoisomerase (reverse gyrase) from an extreme hyperthermophile. *Proc. Natl. Acad. Sci. U.S.A.*, **93**, 106–110.
12. Krah,R., O'Dea,M.H. and Gellert,M. (1997) Reverse gyrase from *Methanopyrus kandleri*. Reconstitution of an active extremozyme from its two recombinant subunits. *J. Biol. Chem.*, **272**, 13986–13990.
13. Rodriguez,A.C. and Stock,D. (2002) Crystal structure of reverse gyrase: insights into the positive supercoiling of DNA. *EMBO J.*, **21**, 418–426.
14. Rodriguez,A.C. (2003) Investigating the role of the latch in the positive supercoiling mechanism of reverse gyrase. *Biochemistry*, **42**, 5993–6004.
15. Rodriguez,A.C. (2002) Studies of a positive supercoiling machine. Nucleotide hydrolysis and a multifunctional "latch" in the mechanism of reverse gyrase. *J. Biol. Chem.*, **277**, 29865–29873.
16. Capp,C., Qian,Y., Sage,H., Huber,H. and Hsieh,T.S. (2010) Separate and combined biochemical activities of the subunits of a naturally split reverse gyrase. *J. Biol. Chem.*, **285**, 39637–39645.
17. Jamroze,A., Perugino,G., Valenti,A., Rashid,N., Rossi,M., Akhtar,M. and Ciaramella,M. (2014) The reverse gyrase from Pyrobaculum calidifontis, a novel extremely thermophilic DNA topoisomerase endowed with DNA unwinding and annealing activities. *J. Biol. Chem.*, **289**, 3231–3243.
18. Andera,L., Mikulika,K. and Savelyevab,N.D. (1993) Characterization of a reverse gyrase from the extremely thermophilic hydrogen-oxidizing eubacterium *Calderobacterium hydrogenophilum*. *FEMS Microbiol. Lett.*, **110**, 107–112.
19. Li,J., Liu,J., Zhou,J. and Xiang,H. (2011) Functional evaluation of four putative DNA-binding regions in Thermoanaerobacter tengcongensis reverse gyrase. *Extremophiles*, **15**, 281–291.
20. Bouthier de la Tour,C., Portemer,C., Kaltoum,H. and Duguet,M. (1998) Reverse gyrase from the hyperthermophilic bacterium *Thermotoga maritima*: properties and gene structure. *J. Bacteriol.*, **180**, 274–281.
21. Brochier-Armanet,C. and Forterre,P. (2007) Widespread distribution of archaeal reverse gyrase in thermophilic bacteria suggests a complex history of vertical inheritance and lateral gene transfers. *Archaea*, **2**, 83–93.
22. Hsieh,T.S. and Capp,C. (2005) Nucleotide- and stoichiometry-dependent DNA supercoiling by reverse gyrase. *J. Biol. Chem.*, **280**, 20467–20475.
23. del Toro Duany,Y.D., Ganguly,A. and Klostermeier,D. (2014) Differential contributions of the latch in Thermotoga maritima reverse gyrase to binding of single-stranded DNA before and after ATP hydrolysis. *Biol. Chem.*, **395**, 83–93.
24. Ganguly,A., del Toro Duany,Y. and Klostermeier,D. (2013) Reverse gyrase transiently unwinds double-stranded DNA in an ATP-dependent reaction. *J. Mol. Biol.*, **425**, 32–40.
25. Rudolph,M.G., del Toro Duany,Y., Jungblut,S.P., Ganguly,A. and Klostermeier,D. (2013) Crystal structures of *Thermotoga maritima* reverse gyrase: inferences for the mechanism of positive DNA supercoiling. *Nucleic Acids Res.*, **41**, 1058–1070.
26. del Toro Duany,Y. and Klostermeier,D. (2011) Nucleotide-driven conformational changes in the reverse gyrase helicase-like domain couple the nucleotide cycle to DNA processing. *Phys. Chem. Chem. Phys.*, **13**, 10009–10019.
27. del Toro Duany,Y., Rudolph,M.G. and Klostermeier,D. (2011) The conformational flexibility of the helicase-like domain from *Thermotoga maritima* reverse gyrase is restricted by the topoisomerase domain. *Biochemistry*, **50**, 5816–5823.
28. Ganguly,A., del Toro Duany,Y., Rudolph,M.G. and Klostermeier,D. (2010) The latch modulates nucleotide and DNA binding to the helicase-like domain of *Thermotoga maritima* reverse gyrase and is required for positive DNA supercoiling. *Nucleic Acids Res.*, **39**, 1789–1800.
29. del Toro Duany,Y., Jungblut,S.P., Schmidt,A.S. and Klostermeier,D. (2008) The reverse gyrase helicase-like domain is a nucleotide-dependent switch that is attenuated by the topoisomerase domain. *Nucleic Acids Res.*, **36**, 5882–5895.
30. Jungblut,S.P. and Klostermeier,D. (2007) Adenosine 5′-*O*-(3-thio)triphosphate (ATPgammaS) promotes positive supercoiling of DNA by *T. maritima* reverse gyrase. *J. Mol. Biol.*, **371**, 197–209.
31. Bouthier de la Tour,C., Amrani,L., Cossard,R., Neuman,K., Serre,M.C. and Duguet,M. (2008) Mutational analysis of the helicase-like domain of *Thermotoga maritima* reverse gyrase. *J. Biol. Chem.*, **283**, 27395–27402.
32. Atomi,H., Matsumi,R. and Imanaka,T. (2004) Reverse gyrase is not a prerequisite for hyperthermophilic life. *J. Bacteriol.*, **186**, 4829–4833.
33. Marguet,E. and Forterre,P. (1994) DNA stability at temperatures typical for hyperthermophiles. *Nucleic Acids Res.*, **22**, 1681–1686.
34. Charbonnier,F. and Forterre,P. (1994) Comparison of plasmid DNA topology among mesophilic and thermophilic eubacteria and archaebacteria. *J. Bacteriol.*, **176**, 1251–1259.
35. Guipaud,O., Marguet,E., Noll,K.M., de la Tour,C.B. and Forterre,P. (1997) Both DNA gyrase and reverse gyrase are present in the hyperthermophilic bacterium *Thermotoga maritima*. *Proc. Natl. Acad. Sci. U.S.A.*, **94**, 10606–10611.
36. Lopez-Garcia,P., Forterre,P., van der Oost,J. and Erauso,G. (2000) Plasmid pGS5 from the hyperthermophilic archaeon *Archaeoglobus profundus* is negatively supercoiled. *J. Bacteriol.*, **182**, 4998–5000.
37. Forterre,P. (2002) A hot story from comparative genomics: reverse gyrase is the only hyperthermophile-specific protein. *Trends Genet.*, **18**, 236–237.
38. Hsieh,T.S. and Plank,J.L. (2006) Reverse gyrase functions as a DNA renaturase: annealing of complementary single-stranded circles and positive supercoiling of a bubble substrate. *J. Biol. Chem.*, **281**, 5640–5647.
39. Kampmann,M. and Stock,D. (2004) Reverse gyrase has heat-protective DNA chaperone activity independent of supercoiling. *Nucleic Acids Res.*, **32**, 3537–3545.
40. Valenti,A., Napoli,A., Ferrara,M.C., Nadal,M., Rossi,M. and Ciaramella,M. (2006) Selective degradation of reverse gyrase and DNA fragmentation induced by alkylating agent in the archaeon *Sulfolobus solfataricus*. *Nucleic Acids Res.*, **34**, 2098–2108.
41. Valenti,A., Perugino,G., Nohmi,T., Rossi,M. and Ciaramella,M. (2009) Inhibition of translesion DNA polymerase by archaeal reverse gyrase. *Nucleic Acids Res.*, **37**, 4287–4295.
42. Napoli,A., Valenti,A., Salerno,V., Nadal,M., Garnier,F., Rossi,M. and Ciaramella,M. (2004) Reverse gyrase recruitment to DNA after

UV light irradiation in *Sulfolobus solfataricus*. *J. Biol. Chem.*, **279**, 33192–33198.
43. Confalonieri,F., Elie,C., Nadal,M., de La Tour,C., Forterre,P. and Duguet,M. (1993) Reverse gyrase: a helicase-like domain and a type I topoisomerase in the same polypeptide. *Proc. Natl. Acad. Sci. U.S.A.*, **90**, 4753–4757.
44. Forterre,P., Gribaldo,S., Gadelle,D. and Serre,M.C. (2007) Origin and evolution of DNA topoisomerases. *Biochimie*, **89**, 427–446.
45. Declais,A.C., Marsault,J., Confalonieri,F., de La Tour,C.B. and Duguet,M. (2000) Reverse gyrase, the two domains intimately cooperate to promote positive supercoiling. *J. Biol. Chem.*, **275**, 19498–19504.
46. Valenti,A., Perugino,G., D'Amaro,A., Cacace,A., Napoli,A., Rossi,M. and Ciaramella,M. (2008) Dissection of reverse gyrase activities: insight into the evolution of a thermostable molecular machine. *Nucleic Acids Res.*, **36**, 4587–4597.
47. Heine,M. and Chandra,S.B. (2009) The linkage between reverse gyrase and hyperthermophiles: a review of their invariable association. *J. Microbiol.*, **47**, 229–234.
48. Perugino,G., Valenti,A., D'Amaro,A., Rossi,M. and Ciaramella,M. (2009) Reverse gyrase and genome stability in hyperthermophilic organisms. *Biochem. Soc. Trans.*, **37**, 69–73.
49. Nadal,M. (2007) Reverse gyrase: an insight into the role of DNA-topoisomerases. *Biochimie*, **89**, 447–455.
50. D'Amaro,A., Rossi,M. and Ciaramella,M. (2007) Reverse gyrase: an unusual DNA manipulator of hyperthermophilic organisms. *Ital. J. Biochem.*, **56**, 103–109.
51. Lima,C.D., Wang,J.C. and Mondragon,A. (1994) Three-dimensional structure of the 67K N-terminal fragment of *E. coli* DNA topoisomerase I. *Nature*, **367**, 138–146.
52. Mondragon,A. and DiGate,R. (1999) The structure of *Escherichia coli* DNA topoisomerase III. *Struct. Fold. Des.*, **7**, 1373–1383.
53. Matoba,K., Mayanagi,K., Nakasu,S., Kikuchi,A. and Morikawa,K. (2002) Three-dimensional electron microscopy of the reverse gyrase from *Sulfolobus tokodaii*. *Biochem. Biophys. Res. Commun.*, **297**, 749–755.
54. Krishna,S.S., Majumdar,I. and Grishin,N.V. (2003) Structural classification of zinc fingers: survey and summary. *Nucleic Acids Res.*, **31**, 532–550.
55. Tanner,N.K. (2003) The newly identified Q motif of DEAD box helicases is involved in adenine recognition. *Cell Cycle*, **2**, 18–19.
56. Andersen,C.B., Ballut,L., Johansen,J.S., Chamieh,H., Nielsen,K.H., Oliveira,C.L., Pedersen,J.S., Seraphin,B., Le Hir,H. and Andersen,G.R. (2006) Structure of the exon junction core complex with a trapped DEAD-box ATPase bound to RNA. *Science*, **313**, 1968–1972.
57. Nielsen,K.H., Chamieh,H., Andersen,C.B., Fredslund,F., Hamborg,K., Le Hir,H. and Andersen,G.R. (2008) Mechanism of ATP turnover inhibition in the EJC. *RNA*, **15**, 67–75.
58. Andreou,A.Z. and Klostermeier,D. (2012) Conformational changes of DEAD-box helicases monitored by single molecule fluorescence resonance energy transfer. *Methods Enzymol.*, **511**, 75–109.
59. Liu,L.F. and Wang,J.C. (1987) Supercoiling of the DNA template during transcription. *Proc. Natl. Acad. Sci. U.S.A.*, **84**, 7024–7027.
60. Jaxel,C., Nadal,M., Mirambeau,G., Forterre,P., Takahashi,M. and Duguet,M. (1989) Reverse gyrase binding to DNA alters the double helix structure and produces single-strand cleavage in the absence of ATP. *EMBO J.*, **8**, 3135–3139.
61. Hsieh,T.S. and Plank,J.L. (2009) Helicase-appended topoisomerases: new insight into the mechanism of directional strand-transfer. *J. Biol. Chem.*, **284**, 30737–30741.
62. Sengoku,T., Nureki,O., Nakamura,A., Kobayashi,S. and Yokoyama,S. (2006) Structural basis for RNA unwinding by the DEAD-box protein *Drosophila* Vasa. *Cell*, **125**, 287–300.
63. Linder,P., Lasko,P.F., Ashburner,M., Leroy,P., Nielsen,P.J., Nishi,K., Schnier,J. and Slonimski,P.P. (1989) Birth of the DEAD-box. *Nature*, **337**, 121–122.
64. Linder,P. and Jankowsky,E. (2011) From unwinding to clamping—the DEAD-box RNA helicase family. *Nat. Rev. Mol. Cell Biol.*, **12**, 505–516.
65. Aregger,R. and Klostermeier,D. (2009) The DEAD-box helicase YxiN maintains a closed conformation during ATP hydrolysis. *Biochemistry*, **48**, 10679–10681.
66. Karow,A.R. and Klostermeier,D. (2009) A conformational change in the helicase core is necessary but not sufficient for RNA unwinding by the DEAD-box helicase YxiN. *Nucleic Acids Res.*, **37**, 4464–4471.
67. Theissen,B., Karow,A.R., Kohler,J., Gubaev,A. and Klostermeier,D. (2008) Cooperative binding of ATP and RNA induces a closed conformation in a DEAD-box RNA helicase. *Proc. Natl. Acad. Sci. U.S.A.*, **105**, 548–553.
68. Henn,A., Cao,W., Hackney,D.D. and De La Cruz,E.M. (2008) The ATPase cycle mechanism of the DEAD-box rRNA helicase, DbpA. *J. Mol. Biol.*, **377**, 193–205.
69. Kelley,L.A. and Sternberg,M.J. (2009) Protein structure prediction on the Web: a case study using the Phyre server. *Nat. Protoc.*, **4**, 363–371.
70. Kirkegaard,K. and Wang,J.C. (1985) Bacterial DNA topoisomerase I can relax positively supercoiled DNA containing a single-stranded loop. *J. Mol. Biol.*, **185**, 625–637.
71. Declais,A.C., de La Tour,C.B. and Duguet,M. (2001) Reverse gyrases from bacteria and archaea. *Methods Enzymol.*, **334**, 146–162.
72. Larkin,M.A., Blackshields,G., Brown,N.P., Chenna,R., McGettigan,P.A., McWilliam,H., Valentin,F., Wallace,I.M., Wilm,A., Lopez,R. *et al.* (2007) Clustal W and Clustal X version 2.0. *Bioinformatics*, **23**, 2947–2948.